



NRC Publications Archive Archives des publications du CNRC

Development and characterization of PEEK/carbon nanotube composites

Díez-Pascual, Ana M.; Naffakh, Mohammed; Gómez, Marián A.; Marco, Carlos; Ellis, Gary; Martínez, Teresa M.; Ansón, Alejandro; González-Domínguez, José M.; Martínez-Rubi, Yadienka; Simard, Benoit

This publication could be one of several versions: author's original, accepted manuscript or the publisher's version. / La version de cette publication peut être l'une des suivantes : la version prépublication de l'auteur, la version acceptée du manuscrit ou la version de l'éditeur.

For the publisher's version, please access the DOI link below. / Pour consulter la version de l'éditeur, utilisez le lien DOI ci-dessous.

Publisher's version / Version de l'éditeur:

<https://doi.org/10.1016/j.carbon.2009.07.020>

Carbon, 47, 13, pp. 3079-3090, 2009-11-01

NRC Publications Record / Notice d'Archives des publications de CNRC:

<https://nrc-publications.canada.ca/eng/view/object/?id=96057940-149c-4d44-b210-d1636d7b26ff>

<https://publications-cnrc.canada.ca/fra/voir/objet/?id=96057940-149c-4d44-b210-d1636d7b26ff>

Access and use of this website and the material on it are subject to the Terms and Conditions set forth at

<https://nrc-publications.canada.ca/eng/copyright>

READ THESE TERMS AND CONDITIONS CAREFULLY BEFORE USING THIS WEBSITE.

L'accès à ce site Web et l'utilisation de son contenu sont assujettis aux conditions présentées dans le site

<https://publications-cnrc.canada.ca/fra/droits>

LISEZ CES CONDITIONS ATTENTIVEMENT AVANT D'UTILISER CE SITE WEB.

Questions? Contact the NRC Publications Archive team at

PublicationsArchive-ArchivesPublications@nrc-cnrc.gc.ca. If you wish to email the authors directly, please see the first page of the publication for their contact information.

Vous avez des questions? Nous pouvons vous aider. Pour communiquer directement avec un auteur, consultez la première page de la revue dans laquelle son article a été publié afin de trouver ses coordonnées. Si vous n'arrivez pas à les repérer, communiquez avec nous à PublicationsArchive-ArchivesPublications@nrc-cnrc.gc.ca.



available at www.sciencedirect.comjournal homepage: www.elsevier.com/locate/carbon

Development and characterization of PEEK/carbon nanotube composites

Ana M. Díez-Pascual^{a,*}, Mohammed Naffakh^a, Marián A. Gómez^a, Carlos Marco^a, Gary Ellis^a, M. Teresa Martínez^b, Alejandro Ansón^b, José M. González-Domínguez^b, Yadienka Martínez-Rubi^c, Benoit Simard^c

^aDepartamento de Física e Ingeniería de Polímeros. Instituto de Ciencia y Tecnología de Polímeros, CSIC, c/ Juan de la Cierva 3, 28006 Madrid, Spain

^bInstituto de Carboquímica, CSIC, c/ Miguel Luesma Castan 4, 50018 Zaragoza, Spain

^cSteacie Institute for Molecular Sciences, NRC, 100 Sussex Drive, Ottawa, Canada

ARTICLE INFO

Article history:

Received 4 February 2009

Accepted 3 July 2009

Available online 9 July 2009

ABSTRACT

New poly(ether ether ketone) (PEEK) based composites have been fabricated by the incorporation of single-walled carbon nanotubes (SWCNTs) using melt processing. Their structure, morphology, thermal and mechanical properties have been investigated. Scanning electron microscopy observations demonstrated a more uniform distribution of the CNTs for samples prepared following a processing route based on polymer ball milling and CNT dispersion in ethanol media. Thermogravimetric analysis indicated a remarkable improvement in the thermal stability of the matrix by the incorporation of SWCNTs. Differential scanning calorimetry showed a decrease in the crystallization temperature with increasing SWCNT content, whilst no significant changes were observed in the melting of the composites. The crystallite size determined by X-ray diffraction decreased at high SWCNT loading, which is attributed to the spatial limitations on crystal growth by confinement within the CNT network. Dynamic mechanical analysis revealed an increase in the storage moduli, hence in the rigidity of the systems, with increasing SWCNT content. Their addition shifts the glass transition peak to higher temperatures due to the restriction in chain mobility imposed by the CNTs. Higher thermal stability and mechanical strength were found for composites with improved dispersion of the SWCNTs.

© 2009 Elsevier Ltd. All rights reserved.

1. Introduction

Over recent years composite materials, especially those involving carbon structures as reinforcement inside a polymer matrix, have become the focus of considerable research [1,2]. In particular, the exceptional properties reported for carbon nanotubes [3,4] (CNTs) have motivated the development of new nanotube-based composites. In addition to their un-

ique mechanical properties [5,6], which combined with their high aspect ratio and nanoscale dimensions makes them excellent candidates for composite reinforcement, they also possess superior thermal and electrical properties [7]. Therefore, polymer-nanotube composites are expected to have many potential applications in several fields: the addition of CNTs could improve thermal transport properties of the polymer, being useful as connectors, thermal interface materials

* Corresponding author. Fax: +34 915 644 853.

E-mail address: adiez@ictp.csic.es (A.M. Díez-Pascual).

0008-6223/\$ - see front matter © 2009 Elsevier Ltd. All rights reserved.

doi:10.1016/j.carbon.2009.07.020

and heat sinks. Alignment of CNTs under a magnetic field leads to an increase in the electric conductivity, so they can be applied in electronic packaging, self-regulating heaters and PTC resistors [8]. Furthermore, incorporation of CNTs into a polymer matrix can provide structural materials with dramatically increased modulus and strength [9]. This behaviour combined with their low density makes them suitable for the transport industry, especially for aerospace structures, where the reduction of weight is one of the main goals in order to reduce fuel consumption. Nowadays the use of polymer composites in the aeronautic industry is mostly associated with secondary parts of the aircraft. Nevertheless, they are starting to be used in structural components, such as wing panels, horizontal and vertical stabilizers and some elements of the fuselage, in order to minimize fuel and manufacturing costs. For this purpose, materials easily processed by continuous methods should be employed; poly(ether ether ketone) (PEEK) carbon nanotube reinforced composites seem to be highly suitable candidates, due to the thermal environment and mechanical requirements of those parts.

PEEK is a semi-crystalline thermoplastic polymer with excellent thermal and chemical stability [10], currently used in a wide range of applications [11], especially for the automobile and aerospace industries. Since its commercialization in 1981, many studies have been reported on the structural [12], thermal [13] and mechanical [14] characterization of this high-performance thermoplastic material. In the literature there are many reports related to the integration of SWCNTs into polymer matrices [15,16], but only a few papers deal with such composites with a PEEK matrix; the most relevant being those published by Shaffer and co-workers [17,18], working with carbon nanofibres/PEEK composites and by Baaba et al. [19], dealing with multi-walled nanotubes functionalized with sulfonated PEEK.

This study approaches two main objectives: firstly, the development of strategies to efficiently incorporate SWCNTs into the PEEK matrix; uniform CNT dispersion and improved nanotube/matrix interface adhesion are critical issues in the processing of these composites in order to achieve efficient reinforcement. Secondly, the characterization of the PEEK composites. A complete characterization at nano(micro)-scopic and macroscopic scales is fundamental to obtain information on the structural and functional changes induced in the polymer with the addition of SWCNTs. The influence of the preparation and processing conditions, as well as SWCNT concentration on the morphology, thermal and dynamic mechanical properties of the resulting composite materials is analyzed in detail in this work.

2. Experimental

2.1. Materials

The matrix used was a commercially available semi-crystalline poly(ether ether ketone), PEEK 150P, supplied by Victrex plc, UK ($M_w \sim 40,000$ g/mol, $T_g = 147$ °C, $T_m = 345$ °C). This low viscosity grade is the most suitable for potential aircraft applications. The polymer, provided as a coarse powder, was vacuum dried at 120 °C for 4 h, and stored in a dry environment before blending. Arc-grown SWCNTs were synthesized by the Institute of Carbon Chemistry (ICB-CSIC), Zaragoza, Spain, using Ni/Y $\sim 2/0.5$ atomic ratio as catalyst according to the procedure reported elsewhere [20]. In order to decrease the metal catalyst content (~ 13 wt% Ni, Y) and to remove amorphous carbon particles, these arc-grown SWCNTs were treated in a reflux of HNO₃ 1.5 M, at 150 °C for 2 h, and then centrifuged at 10,000 rpm for 4 h. This process reduced their metal content by approximately 75%, which demonstrates the effectiveness of the purification step. During the treatment, oxygenated groups are formed, which increase the reactivity of the CNTs, and therefore improve their ability to anchor to the polymer matrix. Laser-grown SWCNTs were prepared by the Steacie Institute for Molecular Sciences (SIMS-NRC), Canada. The residual catalyst (Ni, Co) was lower than 4 wt%, and they were used without further purification. Before proceeding to the fabrication of the composites, arc and laser SWCNTs were characterized by SEM, NIR, FT-Raman spectroscopy and TGA; these results are detailed in another section.

2.2. Preparation of PEEK/SWCNT composites

To verify the potential improvement in the CNT dispersion caused by a pre-processing step based on mechanical treatments in alcohol media, and its possible influence on the properties of the composites, we have prepared PEEK/SWCNT systems following two different procedures. As received raw arc-grown and laser-grown SWCNTs (named ZC1 and LC1, see nomenclature in Table 1) were directly mixed with dried PEEK powder. Purified arc-grown and laser-grown SWCNTs (named ZC1p and LC1m, respectively) were integrated in the matrix as follows: firstly, PEEK polymer was ground with a ball mill in order to reduce its particle size. Secondly, the polymer was mixed with different amounts of CNTs. Each mixture PEEK/SWCNT was then dispersed in 30 mL of ethanol and sonicated in an ultrasonic bath for 30 min. Subsequently, the dispersion was partially dried under vacuum (70 mbar)

Table 1 – Characteristics and codes of the SWCNTs used for the preparation of the composites.

Preparation method	Metal (%) (TGA)	T_{mr} (°C) (TGA)	G/D ratio (Raman)	Purity (%) (NIR)	D (nm) SEM	Sample code
Arc (as-grown)	12.7	459	5.6	35.7	21.8	ZC1
Arc (HNO ₃ treated)	3.2	541	14.3	50.4	20.4	ZC1p
Laser (as-grown)	3.9	493	7.2	38.8	39.8	LC1 and LC1m

T_{mr} corresponds to the temperature of maximum rate of weight loss under air atmosphere, and D to the average bundle diameter obtained by SEM micrographs.

ZC1p and LC1m SWCNTs were integrated in the matrix following a pre-processing step based on ball milling and premixing under mechanical treatments in ethanol (see explanation in the text).

at 50 °C for 5 min, sonicated for another 30 min, and heated until the ethanol was completely eliminated.

All types of PEEK/SWCNT composites studied in this work, containing concentrations of 0.1, 0.5 and 1 wt% SWCNTs, were prepared by melt-blending in a Thermo-Haake MiniLab micro-extruder, at 380 °C, using 5 g of total material, with a rotor speed of 150 rpm. Mixing times of 20 min were applied, selected as standard conditions according to preliminary tests. Homogeneous films were prepared in a Collin press at 380 °C under 130 bar and cooled between aluminium plates at 15 °C. Samples were annealed for 3 h at 200 °C to increase their crystallinities.

2.3. FT-Raman spectroscopy

The FT-Raman Spectra of the SWCNTs were performed with a Perkin–Elmer System 2000R, using a Nd:YAG laser excitation source (1064 nm), and an InGaAs detector operating at room temperature. To improve the signal-to-noise ratios, spectra were recorded with an incident laser power of 25 mW and resolution of 4 cm⁻¹.

2.4. Near infrared spectroscopy

A Perkin–Elmer Lambda 900 UV–VIS–NIR spectrophotometer was used to obtain NIR spectra of the SWCNTs, in the wave-number range between 6000 and 14,000 cm⁻¹. The SWCNTs were homogenized and dispersed in DMF by use of an ultrasonic bath. The solution was diluted until a final concentration of approximately 0.01 mg/mL was reached. The samples were sonicated just before the spectral measurement in order to assure high quality dispersion.

2.5. Thermogravimetric analysis

The thermal stability of the SWCNTs and the composites was analyzed by thermogravimetric analysis (TGA). The measurements were carried out using a TA-Q500 thermobalance, at heating rate of 10 °C/min, under nitrogen and dry air atmospheres. The analysis was performed on samples with an average mass of 10 mg, under dynamic conditions, from room temperature to 900 °C, with a gas purge of 150 mL/min. Before the measurements, treated SWCNTs were dried overnight at 100 °C to assure total evaporation of the solvent.

2.6. Differential scanning calorimetry

The crystallization and melting behaviour of the composites were investigated by DSC using a Mettler TA 400/DSC 30 differential scanning calorimeter, operating under nitrogen flow. Samples of approximately 10 mg were weighed and sealed in aluminium sample pans. Before the heating and cooling scans, composites were melted at 380 °C and maintained at this temperature for 5 min in order to erase the thermal history of the material. Subsequently they were cooled from 380 to 30 °C at a rate of 10 °C/min, and then heated from 30 to 380 °C at 10 °C/min.

The transition temperatures were taken as the peak maximum or minimum in the calorimetric curves. The levels of

crystallinity of PEEK composites were determined using the following relation: $(1 - \lambda)_m = \Delta H_{m,PEEK} / (\Delta H_{m,PEEK}^0 \times w_{PEEK})$, where $\Delta H_{m,PEEK}$ is the apparent melting enthalpy of PEEK, w_{PEEK} is the weight fraction of PEEK in the composites and $\Delta H_{m,PEEK}^0$ is the extrapolated value of the enthalpy corresponding to the melting of a 100% crystalline sample, taken as 130 J/g [21].

2.7. X-ray diffraction

Measurements were performed in a D8 Advanced Bruker Instrument, equipped with a Göbel mirror and a Vantec PSD detector, with a voltage of 40 kV and an intensity of 40 mA, using Cu K α ($\lambda = 0.15418$ nm) radiation, with an aperture of 0.6 mm. Diffractograms were registered on films or powder, in the angular region of $2\theta = 5\text{--}40^\circ$, at room temperature, with a scan speed of 0.2 s and angular increment of 0.02°.

2.8. Scanning electron microscopy

SEM measurements were performed with a Philips XL 30 ESEM microscope using a voltage of 25 kV and an intensity of 9×10^{-9} A. In order to avoid charging during electron irradiation, the composite film samples were fractured in liquid nitrogen and covered with an approximately 5 nm overlayer of an Au–Pd (80–20) alloy in Balzers SDC 004 evaporator, using a covering time of 242 s at 20 mA. At least 10 SEM images of each composite sample were taken at different magnifications to assess the state of dispersion of the CNTs in the PEEK matrix.

2.9. Dynamic mechanical analysis

The dynamic mechanical performance of the composites was studied using a Mettler DMA 861 dynamic mechanical analyzer. Rectangular shaped samples of $\sim 19.5 \times 4 \times 0.5$ mm³ were mounted in a large tension clamp. The measurements were performed in the tensile mode at frequencies of 0.1, 1 and 10 Hz, in the temperature range between –130 and 260 °C, at heating rate of 2 °C/min. A dynamic force of 6 N was used oscillating at fixed frequency and amplitude of 30 μ m.

3. Results and discussion

3.1. Characterization of the single-walled carbon nanotubes

A complete characterization of all SWCNTs used was performed before the preparation of the composites; these results are summarized in Table 1.

The FT-Raman spectra of the SWCNTs were recorded in order to analyze their most characteristic bands. As an example, Fig. 1 presents the spectra of purified arc-grown SWCNTs, where four main bands can be observed [22]: the tangential G band, whose profile reveals the semiconductor character, the disorder induced D band, G' band (D overtone) and the radial breathing modes. The relative purity represented by the G/D intensity ratio [23] is listed in Table 1.

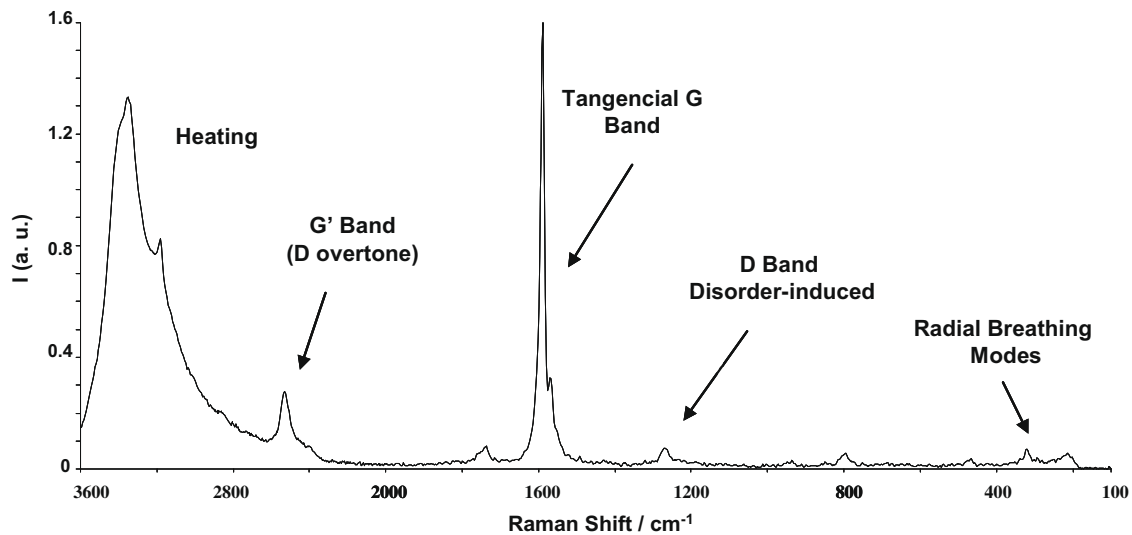


Fig. 1 – FT-Raman spectra of arc-grown SWCNTs (ZC1p), with a laser output of 25 mW and resolution of 4 cm^{-1} .

The quality of the nanotubes was analyzed by NIR spectroscopy, following the method described by Itkis et al. [24]. NIR spectra of laser SWCNTs dispersed in DMF is shown in Fig. 2. The S_{11} peak for arc-produced SWCNTs is typically located between 5000 and 7000 cm^{-1} [25]; the high-energy edge of this absorption peak is just visible in the spectrum. The S_{22} transition of semiconducting SWCNTs can be clearly observed. The ratio between the S_{22} peak area after baseline correction and the S_{22} total area indicates the purity of the material; calculated values are included in Table 1. As expected, purified arc-grown SWCNTs show higher purity than raw ones; this evidences again the effectiveness of the purification step.

SEM images of arc-grown SWCNTs (not shown) revealed a high degree of agglomeration, with an average bundle diameter of 21.8 nm (see Table 1). Residual impurities could be observed in the micrographs, which were effectively removed after the purification process. Laser SWCNTs also appeared quite agglomerated, with average bundle diameter of 39.8 nm . However, taking into account the non-homogeneous

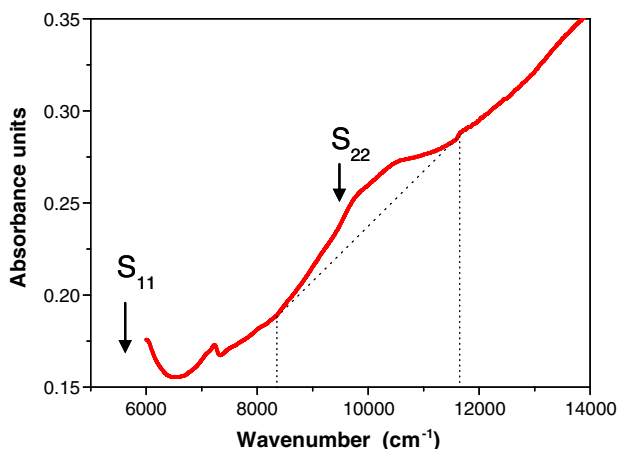


Fig. 2 – NIR spectra of laser-grown SWCNTs (LC1) dispersed in DMF, with a concentration of approximately 0.01 mg/mL .

size distribution of the diameters revealed by the micrographs and the detection limit of the technique (about 20 nm), these should be considered only as approximated values.

In order to analyze the thermal behaviour of the SWCNTs and to determine their metallic residue, TGA under dry air conditions was carried out. All thermograms present only one decomposition step, with a small amount of residue left due to the catalyst used in the synthesis. It is well known that CNTs exhibit very high thermal stability [26]; however, temperatures for the maximum rate of oxidation can vary by up to $\pm 100\text{ }^{\circ}\text{C}$ depending on sample preparation, treatment as well as the metallic content that catalyzed the thermal oxidation. Our results revealed temperatures of maximum weight loss ranging between $459\text{ }^{\circ}\text{C}$, for raw arc-grown SWCNTs, and $541\text{ }^{\circ}\text{C}$, for purified arc-grown SWCNTs (see Table 1). According to literature [27], other forms of disordered carbon present significantly lower temperatures of maximum degradation than CNTs; this could explain the fact that purified SWCNTs decompose at temperatures $\sim 80\text{ }^{\circ}\text{C}$ higher than as prepared SWCNTs. TGA experiments were also performed in a N_2 atmosphere, where the SWCNT degradation initiates at temperatures well above $600\text{ }^{\circ}\text{C}$. Under inert conditions they are thermally more stable than in an oxidative environment, in agreement with TGA studies performed by other authors [28].

3.2. Carbon nanotube dispersion in the composites

To achieve a good dispersion of the SWCNTs in the polymer matrix is the key to fabricate composites with enhanced thermal and mechanical properties. This is commonly a difficult task, because carbon nanotubes have strong tendency to gather and form bundles [29].

In order to assess the state of dispersion and morphology of the fabricated composites, the surfaces of cryofractured films were examined by SEM. Fig. 3 shows typical micrographs of different PEEK/SWCNT systems. Fig. 3a and b compares a composite prepared by direct integration (PEEK/ZC1

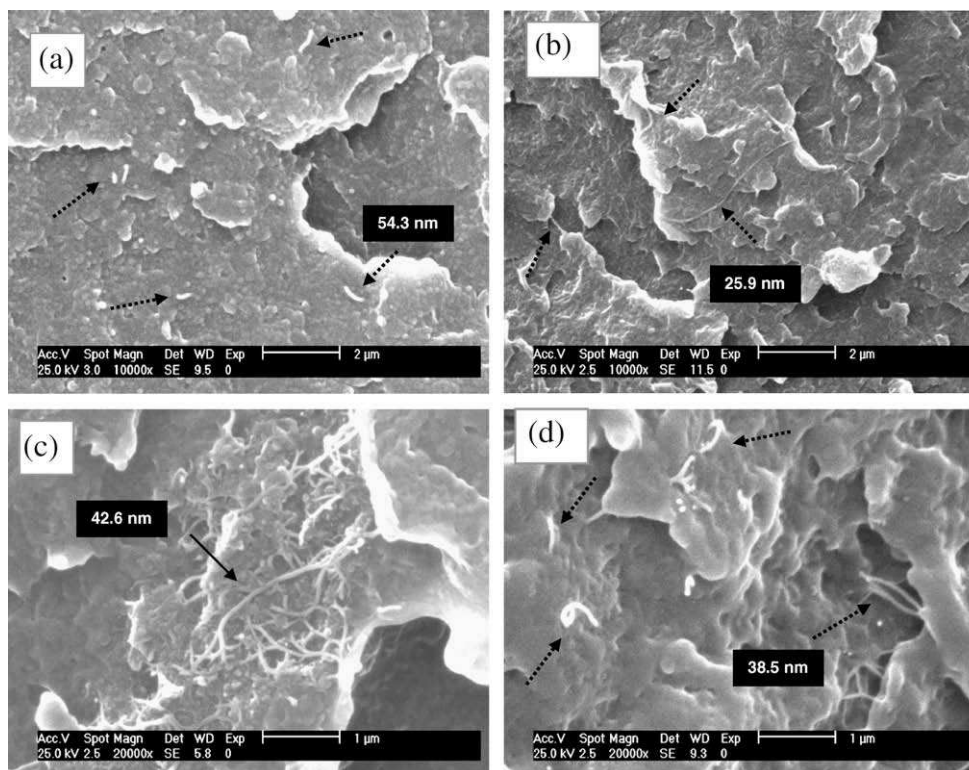


Fig. 3 – SEM micrographs from fractured surfaces of different types of PEEK/SWCNT composites metallised with a ~ 5 nm Au/Pd overlayer. Top panel: comparison between PEEK/ZC1 0.5 wt% (a) and PEEK/ZC1p 0.5 wt% (b). Bottom panel: comparison between PEEK/LC1 1.0 wt% (c) and PEEK/LC1m 1.0 wt% (d). (a) and (c) correspond to composites prepared by direct mixing, whereas composites shown in (b) and (d) were prepared following a pre-processing based on mechanical treatments in ethanol (see explanation in the text). The dashed arrows point out randomly distributed nanotube bundles in the matrix.

0.5 wt%, Fig. 3a), with another obtained following the procedure of dispersion in ethanol (PEEK/ZC1p 0.5 wt%, Fig. 3b). The CNTs, which appear as bright spots (see the arrows marked on the images), seem to be homogeneously dispersed within the PEEK matrix in both types of composites. However, the size of the domains of raw arc-grown SWCNTs is relatively larger, and consequently they are easier to visualize. According to the images, a bundle of ZC1 has approximately twice the diameter of a bundle of ZC1p, meaning that purified SWCNTs are more disentangled and better integrated in the matrix. Samples including both types of SWCNTs show a good interfacial adhesion between the filler and matrix phases, as no open ring holes are found around the nanotubes.

Fig. 3c and d compares composites with 1 wt% laser-grown SWCNTs which only differ in the preparation method. As it can be clearly observed, the SWCNTs are quite agglomerated in the sample prepared by direct mixing (PEEK/LC1, Fig. 3c), and tend to concentrate in certain regions of the matrix, forming a highly entangled interconnected structure. However, the sample fabricated with the aid of mechanical pre-treatments (PEEK/LC1m, Fig. 3d) shows an improved dispersion of the SWCNTs. The size of the domains in the dispersed phase is considerably smaller and CNTs are randomly distributed through the whole matrix. Notice also that the observed bundle diameters for SWCNTs dispersed in ethanol are consistent (within the experimental error) with the values ob-

tained from SEM images of the SWCNTs alone. This indicates that most SWCNTs were separated into smaller bundles by the disentanglement process in ultrasonic bath, and confirms the efficiency of these mechanochemical pre-treatments.

3.3. Thermal stability

To study the thermal stability of the composites, TGA characterization has been carried out under dry air and nitrogen atmospheres. The degradation curves of pure PEEK and composites containing 1 wt% SWCNTs are displayed in Fig. 4. It can be observed that the decomposition under inert environment takes place in a single stage, which involves decarboxylation, decarbonylation and dehydration processes, leading to the formation of phenol groups, carbon dioxide and water [30]. The ether and aromatic structures remain in the residue up to very high temperatures [31]. At 700 °C the residual amount in all composites is approximately 46% of the initial weight. Pure PEEK starts to degrade at 521 °C and shows the maximum rate of weight loss (T_{mr}) at 558 °C. The incorporation of SWCNTs induces a remarkable thermal stabilization of the matrix; thus, the addition of 1 wt% LC1m or ZC1p increases the initial degradation temperature (T_i) up to 25 °C and delays T_{mr} by about 20 °C. However, if we focus on the composites prepared by direct mixing, the increase in the aforementioned temperatures is considerably lower. This

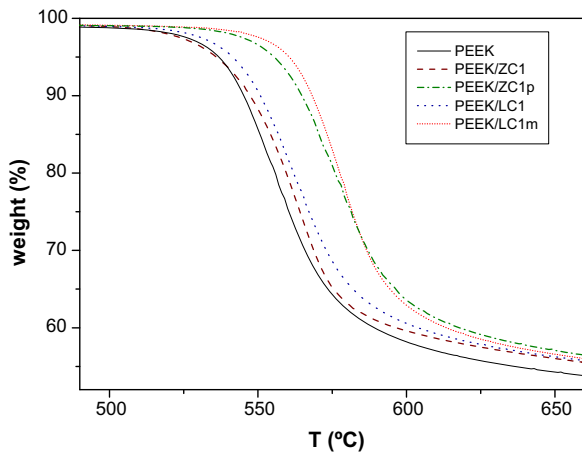


Fig. 4 – TGA curves for different types of 1 wt% PEEK/SWCNT composites in nitrogen atmosphere, at a heating rate of 10 °C/min. For comparative purposes, only the temperature range between 500 and 650 °C is plotted.

observation reveals that a more uniform and fine dispersion of the SWCNTs improves the interfacial adhesion between the CNTs and the matrix and restricts the thermal motion of the PEEK chains, thereby leading to composites thermally more stable. Similar enhancements in the thermal stability attributed to a more homogeneous distribution of the CNTs have been reported for Nylon 6/MWCNT [32] and PU/MWCNT [33] composites.

Apart from the preparation procedure, other factors seem to affect the decomposition process. Samples including raw arc-grown SWCNTs show the lowest degradation temperatures. This is consistent with the results obtained from TGA study of the SWCNTs, which points out that ZC1 is the first to initiate decomposition, probably due to its higher content in metal impurities that catalyze the degradation process. However, small differences are found between T_{mr} of compos-

ites prepared with purified arc-grown and laser-grown SWCNTs, which seems reasonable taking into account their similar content in metal catalysts (see Table 1).

The effect of SWCNT content on the thermal behaviour of the composites can be disclosed from Table 2, which presents the characteristic temperatures for the PEEK/SWCNT systems. Samples with different SWCNT loading begin to lose weight nearly at the same temperature, but the maximum mass loss rate is usually delayed by a few degrees. Hence, if we focus on the PEEK/LC1m system, by incorporating 0.1, 0.5 and 1 wt% SWCNTs, T_{mr} increases by 7, 15 and 19 °C, respectively. This suggests that an increase in the SWCNT content enhances the thermal stability of the composite. Analogous behaviour has been reported in the literature for various polymer/CNT composites [34,35]. The observed stabilization may be attributed to the barrier effect of CNTs, which hinders the diffusion of the degradation products from the bulk of the polymer to the gas phase. Another plausible explanation could be the higher thermal conductivity of the composite that facilitates heat dissipation within the sample.

The behaviour mentioned above does not significantly differ from that found under dry air atmosphere (data not shown). The incorporation of a very small amount of uniformly and well-dispersed SWCNTs also stabilises the composite in an oxidative environment, raising the matrix T_i by an average of 10 °C; the stabilizing effect also affects T_{mr} , which increases progressively as SWCNT loading rises.

3.4. Crystallization behaviour

DSC was employed to evaluate the effect of SWCNTs on the crystallization and melting behaviour of different types of PEEK/SWCNT composites. Fig. 5 shows, as an example, the crystallization exotherms and heating endotherms for films of PEEK and PEEK/LC1m with different SWCNT content. In Fig. 5a it can be observed that the crystallization temperature T_c , obtained from the minimum of the exothermic peak, is about 309 °C for pure PEEK. The incorporation of 0.1–1 wt% SWCNTs leads to a progressive shift of the crystallization peak towards lower temperatures ($T_{c-0.1\text{ wt}\%} = 307.5\text{ °C}$, $T_{c-0.5\text{ wt}\%} = 305.1\text{ °C}$, $T_{c-1\text{ wt}\%} = 303.3\text{ °C}$). However, the apparent crystallization enthalpy ΔH_c , calculated as the normalized integral of the crystallization peak, and therefore the crystallinity remain almost unchanged. These observations are intriguing since nanotubes usually act as nucleating agents [36,37] that increase the crystallization rate, because the nucleation starts simultaneously in multiple centers; therefore one expects a similar if not higher T_c for the composites. This unusual behaviour can be explained by a confinement effect [38]: the CNT network imposes a confinement on polymer chain diffusion and crystal growth which slows down the overall crystallization process, leading to lower values of T_c for the composites. Nevertheless, our results are consistent with the behaviour described by Shaffer and co-workers [18] on DSC analysis of carbon-nanofibre/PEEK composites. A small T_c decrease was observed for samples with nanofibre loading up to 5 wt%, and this effect was attributed to interactions between the matrix and the nanoscale filler occurring during the crystallization process. Furthermore, in other systems such as PPS/IF-WS₂ composites, the crystallization of the

Table 2 – Characteristic temperatures of the PEEK/SWCNT composites obtained from TGA measurements under nitrogen atmosphere at heating rate of 10 °C/min.

Mat. (% SWCNTs)	T_i (°C)	T_{10} (°C)	T_{mr} (°C)
PEEK	521	544	558
PEEK/LC1m (0.1)	542	557	565
PEEK/LC1m (0.5)	544	563	573
PEEK/LC1m (1.0)	546	568	577
PEEK/LC1 (0.1)	523	547	559
PEEK/LC1 (0.5)	525	549	561
PEEK/LC1 (1.0)	526	551	564
PEEK/ZC1p (0.1)	536	550	564
PEEK/ZC1p (0.5)	540	558	574
PEEK/ZC1p (1.0)	543	564	578
PEEK/ZC1 (0.5)	520	545	560
PEEK/ZC1 (1.0)	521	547	562

The displayed temperatures are: T_i : initial degradation temperature obtained at 2% weight loss; T_{10} : temperature for 10% weight loss; T_{mr} : temperature of maximum rate of weight loss.

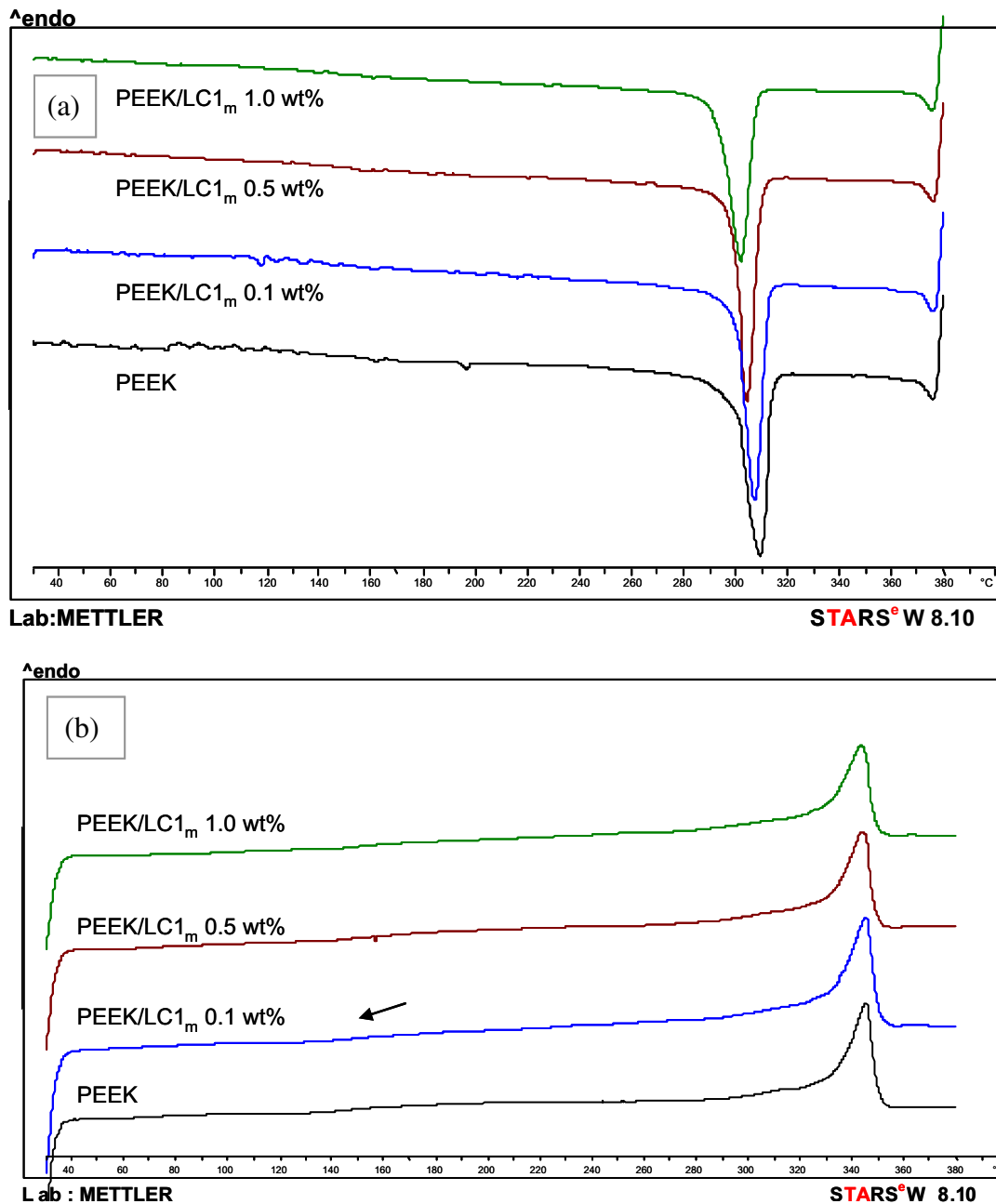


Fig. 5 – Non-isothermal DSC scans of PEEK/LC1m composites at rates of 10 °C/min, for samples with different SWCNT content. (a) Crystallization thermograms. (b) Heating thermograms. The arrow indicates the glass transition of the polymer matrix in the composite.

matrix was found dependent on the IF-WS₂ concentration, but in ways unexpected for polymer blends. A drastic change from retardation to promotion of PPS crystallization was observed depending on the nanoparticle content, which was related to the change in the fold surface free energy [39].

In the case of the melting process, the DSC heating curves in Fig. 5b show an endothermic peak for pure PEEK at 344.2 °C, which corresponds to the melting temperature T_m , and a small variation of the specific heat associated to the glass transition at about 150 °C (this temperature is more accurately determined from DMA measurements). The addition of SWCNTs does not significantly change T_m or the apparent

melting enthalpy ΔH_m , in agreement with the observations reported from heating thermograms of carbon-nanofibre/PEEK composites [18].

The aforementioned behaviour has been systematically found within all PEEK/SWCNT systems, as it can be observed in Table 3, which presents experimental DSC data and the degree of crystallinity of all composites prepared. A close analysis of this table reveals that T_c is not significantly affected by the type of SWCNT. Regarding the influence of the composite fabrication procedure, it is confirmed that samples with improved degree of dispersion of the SWCNTs in the matrix present slightly higher T_c than those obtained by direct

Table 3 – DSC crystallization and melting data of PEEK/SWCNT composites.

Mat. (% SWCNTs)	T_c (°C)	ΔH_c (J/g)	$(1 - \lambda)_c$ (%)	T_m (°C)	ΔH_m (J/g)	$(1 - \lambda)_m$ (%)
PEEK	309.1	55.3	42.5	344.2	58.2	44.8
PEEK/LC1m (0.1)	307.5	57.8	44.5	343.5	58.5	45.0
PEEK/LC1m (0.5)	305.1	56.5	43.7	343.1	57.3	44.3
PEEK/LC1m (1.0)	303.3	54.4	42.3	342.6	55.7	43.2
PEEK/LC1 (0.1)	307.7	56.4	43.4	343.4	58.3	44.9
PEEK/LC1 (0.5)	305.8	55.6	42.9	343.0	58.0	44.8
PEEK/LC1 (1.0)	304.9	53.9	41.8	342.8	55.8	43.3
PEEK/ZC1p (0.1)	308.1	58.2	44.8	343.9	58.6	45.0
PEEK/ZC1p (0.5)	306.6	57.0	44.1	343.2	57.5	44.4
PEEK/ZC1p (1.0)	304.3	54.6	42.3	342.6	56.6	44.0
PEEK/ZC1 (0.5)	304.0	56.4	43.6	343.9	58.5	45.2
PEEK/ZC1 (1.0)	303.1	53.2	41.3	342.3	55.4	43.0

The displayed data are: T_c : crystallization temperature; ΔH_c : apparent crystallization enthalpy; T_m : melting temperature; ΔH_m : apparent melting enthalpy; $(1 - \lambda)_c$ and $(1 - \lambda)_m$: crystallization and melting crystallinities derived from the peak areas.

mixing; in the latter the existence of small agglomerates makes the indicated confinement effect more significant and therefore crystallization occurs at lower temperatures.

In general, differences between the levels of crystallinity of the composites are quite small, lower than 5%. Moreover, over the whole composition range, crystallinity values obtained from the melting curves are slightly higher than those derived from the cooling thermograms. This fact may be due to a recrystallization from defective to more perfect crystals which takes place during the heating.

3.5. Crystalline structure

The crystalline structure of PEEK/SWCNT composites was also characterized using wide angle X-ray diffraction. Four main peaks can be observed at 2θ values of 18.8°, 20.7°, 22.9° and 28.9°, which correspond to the diffraction of the (1 1 0), (1 1 1), (2 0 0) and (2 1 1) crystalline planes [40], respectively, of the orthorhombic unit cell. All composites exhibit similar diffractogram to the PEEK matrix, differing mainly in the width and intensity of the peaks. No shift in the position of the Bragg reflections is observed. As the SWCNT content increases, peaks became wider and with decreased intensity. Composites prepared by dispersion in ethanol show narrower peaks than those obtained by direct mixing.

The crystallite size perpendicular to the diffraction (1 1 0) plane, D_{110} , obtained from the room temperature diffractograms using the Scherrer expression [41], increases with the addition of SWCNTs until a concentration of 0.1 wt% is reached and then slightly decreases. This behaviour can be explained based on the aforementioned confinement effect and the T_c decrease observed from DSC thermograms. The incorporation of very low SWCNT content slightly reduces the crystallization rate of PEEK, leading to the formation of smaller crystals than those of the polymer in the vicinity of T_c . Since the confinement effect is almost insignificant at these concentrations, during the cooling process PEEK crystals grow considerably, resulting in larger room temperature D_{110} values than the calculated for the pure matrix. On contrast, at higher SWCNT loading, the reduction in the crystalli-

zation rate is stronger and on cooling the dense nanotube network imposes a remarkable confinement on crystal growth; therefore, at room temperature samples with high SWCNT concentration present lower crystal size than the matrix. However, to fully confirm this hypothesis, an in-depth understanding of the crystallization processes is required, which is out of the scope of this paper. Regarding to the influence of SWCNT type, it is found that samples containing purified SWCNTs present the highest D_{110} values. Thus, the integration of 0.1 wt% ZC1p increases the crystallite size of the matrix (20.9 nm) by nearly 10%. Moreover, the decrease of the matrix particle size and the procedure of dispersion in ethanol also lead to larger crystals.

3.6. Dynamic mechanical properties

The influence of SWCNT content on the mechanical properties of the composites has been explored by DMA. Fig. 6 shows, as an example, the temperature dependence of the storage modulus (E') and loss modulus (E'') of PEEK and PEEK/LC1m composites, for different SWCNT loading, at the frequency of 1 Hz. Similar dynamic mechanical spectra were recorded for the different samples. The storage modulus of pure PEEK decreases slowly and progressively with increasing temperature, showing a very strong decay (higher than 85%) in the temperature range between 138 and 170 °C, which correlates with the glass transition of the polymer, according to DSC experiments (see Fig. 5b). The loss modulus exhibits a low broad peak around -95 °C and an intense sharp peak at 148.3 °C. The first maximum is generally attributed to the β relaxation [14], associated with local motions of the ketone groups, whereas the second is the α relaxation [42], considered to be the glass transition of the material.

In most of the temperature range, the incorporation of increasing contents of SWCNTs induces a progressive rise in the storage modulus of the matrix. Thus, at room temperature, composites containing 0.1, 0.5 and 1 wt% SWCNTs increased E' by approximately 16, 23 and 27%, respectively. The observed enhancement in the mechanical response is attributed to the effective load transfer from the matrix to

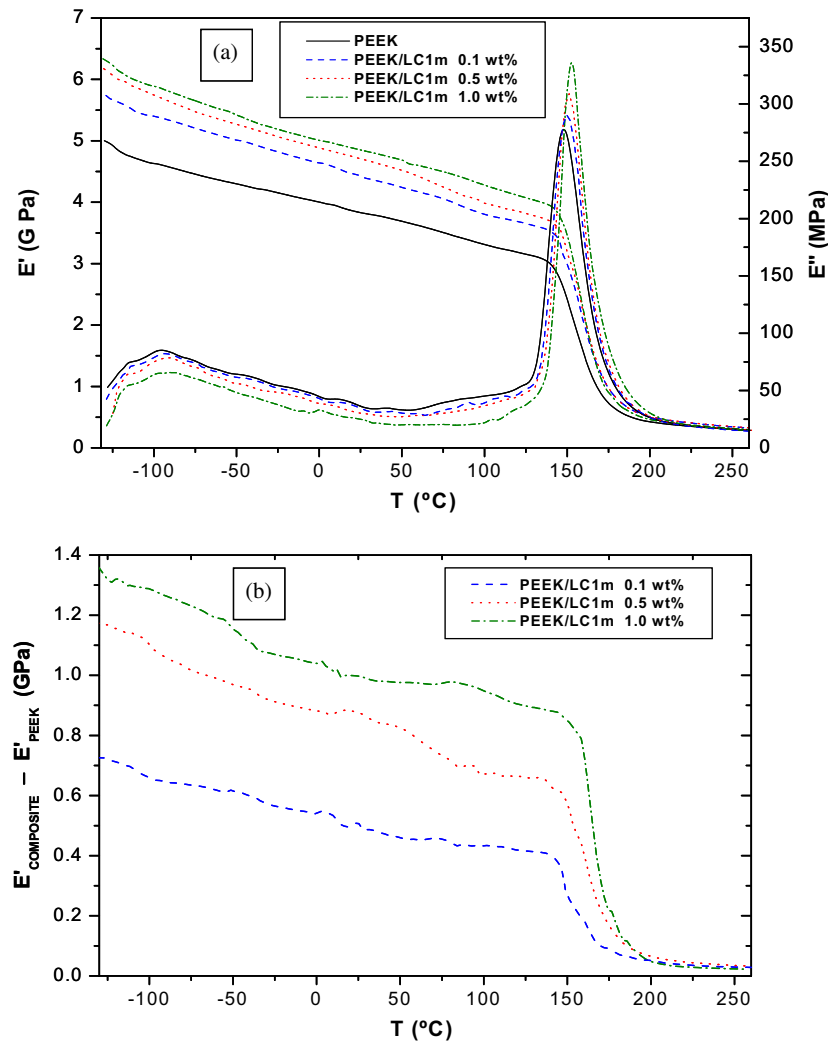


Fig. 6 – (a) Temperature dependence of the storage modulus E' and loss modulus E'' of PEEK/LC1m composites, for different SWCNT content, obtained from DMA measurements at the frequency of 1 Hz. (b) Storage moduli difference between the composites and the pure PEEK as a function of temperature.

the fillers likely resulting from an improvement in the SWCNT dispersion. Analogous behaviour of mechanical enhancement has been reported in the literature for different polymer/SWCNT composites [33,43]. Our experimental data reveal a non-linear growth of E' with SWCNT content, the increase being more pronounced at low concentrations. These results are not consistent with the predictions of continuum-based volume additivity models [44]. E' of samples with 0.1 wt% SWCNTs exceeded the theoretical calculations, whereas those of the other compositions were lower than expected. At very low concentrations, the nanotubes are well dispersed and therefore E' increases rapidly with SWCNT content. However, when the concentration becomes sufficiently large, the nanotubes interact and form small aggregates. CNT agglomeration reduces the aspect (length-to-diameter) ratio and the modulus of the filler and limits the interfacial area for stress transfer to the polymer matrix; this is reflected in E' values which fell appreciably below theoretical predictions. The aforementioned results are in contrast to the study of vapour-grown carbon nanofibres/PEEK compos-

ites [17] prepared by injection moulding, which revealed a linear increase in stiffness with increasing nanofibre loading. This contradictory can be explained based on the large aspect ratio, high mass density and low flexibility of carbon nanofibres compared to CNTs [4] and on the processing routes employed for the transformation of the blends that play a key role in the resulting properties of these materials.

Furthermore, the difference between the storage modulus of the composite ($E'_{\text{composite}}$) and the matrix (E'_{PEEK}), plotted in Fig. 6b, represents the contribution of the nanotubes to the overall modulus; this contribution decreases with increasing temperature, showing a substantial drop around T_g and becomes negligible at higher temperatures. Hence, at -100°C , 1 wt% SWCNT loading contributes ~ 1.3 GPa to the storage modulus, while this contribution is reduced to ~ 1 GPa at 25°C and to ~ 0.04 GPa at 200°C . Considering that SWCNT modulus is not very sensitive to temperature [45], the observed drop in the storage moduli difference suggests highly temperature dependent nature of the load transfer efficiency between the matrix and the reinforcement, hence of the

Table 4 – Storage modulus E' and loss modulus E'' at 25 °C, and glass transition temperatures T_g for the different PEEK/SWCNT composites obtained from dynamic mechanical analysis measurements at the frequency of 1 Hz.

Mat. (% SWCNTs)	E' (GPa)	E'' (MPa)	T_g (°C)	Mat. (% SWCNTs)	E' (GPa)	E'' (MPa)	T_g (°C)
PEEK	3.83	37.2	148.3	PEEK/LC1m (0.1)	4.43	33.1	149.9
PEEK/ZC1p (0.1)	4.20	34.6	151.0	PEEK/LC1m (0.5)	4.71	29.7	152.2
PEEK/ZC1p (0.5)	4.59	31.0	153.3	PEEK/LC1m (1.0)	4.86	25.9	154.0
PEEK/ZC1p (1.0)	4.63	29.5	155.1	PEEK/LC1 (0.1)	3.95	36.7	149.4
PEEK/ZC1 (0.5)	3.98	36.6	150.2	PEEK/LC1 (0.5)	4.11	35.9	151.8
PEEK/ZC1 (1.0)	4.05	36.1	152.6	PEEK/LC1 (1.0)	4.21	34.3	153.5

interfacial strength in these composites. This decrease in load transfer ability as temperature rises can be partially attributed to changes in the PEEK structure and morphology resulting from the presence of SWCNTs. A similar phenomenon for load transfer ability was also observed in composites where the reinforcing entities were spherical particles [46]. The drastic jump of $E'_{\text{composite}} - E'_{\text{PEEK}}$ in the vicinity of T_g was mainly attributed to changes in Poisson's ratio of the polymer as well as to variations in the ratio of the modulus of the filler to that of the matrix when going through the glass transition [47].

With regard to the loss modulus data for different compositions (Fig. 6a), it is evident that the introduction of SWCNTs results in a reduction of E'' magnitude at temperatures below T_g ; the decrease is steeper at extremely low concentrations and gets smoother as the concentration becomes higher. With an increase of SWCNT content, the β relaxation was broadened, smoothed and shifted to higher temperatures; this suggests that the presence of SWCNTs act as a barrier for the local movements of the ketone groups. It can be observed in the figure that the addition of SWCNTs causes small increases in T_g , hence in the stiffness of the systems. Since the glass transition is associated with the mobility of chain segments in the amorphous regions, a likely explanation is that those segments in the vicinity of the nanotubes are less mobile, because CNTs restrict rotational motion within the chains and therefore lead to a raise in T_g . Such effects have been observed in other polymer systems with finely dispersed materials [48].

We have observed that the influence of SWCNTs in the DMA behaviour of the PEEK matrix is the same at other frequencies, with an increase in the storage modulus and in the temperature of the relaxation peaks as frequency is shifted to higher values. For this reason our experimental results are only discussed at 1 Hz.

To study the influence of the processing route on the mechanical response of the composites, the storage modulus E' and loss modulus E'' , at 25 °C, as well as the glass transition T_g of different 1 wt% PEEK/SWCNT composites were compared at the frequency of 1 Hz (see Table 4). As it was expected, composites prepared following the procedure of dispersion in ethanol present higher E' than those obtained by direct mixing. Hence, the former composites increased PEEK modulus between 21% and 27% (which corresponds to the incorporation of ZC1p and LC1m, respectively), whereas for the other samples the increment was lower than 10%. Chen and co-workers illustrated similar effects with MWCNTs in Nylon 6, indicating that the interfacial interaction was more effective in strengthening the material in com-

posites with uniformly dispersed CNTs [32]. Remarkable differences were also found within their glass transition temperatures; T_g increase was more significant in samples with improved SWCNT dispersion. This is consistent with SEM observations: samples prepared by direct mixing are more heterogeneous and CNTs tend to concentrate in certain regions of the matrix, leaving the others with very low reinforcement content. In the latter areas the molecular movements are only partially limited and therefore T_g increment is lower than expected. However, when the SWCNT distribution is homogeneous, the restriction in mobility is almost identical over the whole matrix and consequently T_g rise is higher.

Apart from the preparation procedure, the type of SWCNT also seems to influence the storage modulus of the composites. Thus, for the different CNT loadings tested, it was found that samples including laser-grown SWCNTs exhibit the highest E' . This is not surprising since the purity, quality, aspect ratio and nature of impurities, hence the source of SWCNTs are determining factors in the final properties of CNT based composites. It has recently been shown that defects have detrimental effects on mechanical properties of SWCNTs [49]. The laser process produces CNTs of the highest quality (few defects, high crystallinity) as compared to any other synthesis methods known; it also generates nanotubes with very large aspect ratio (>10,000). Acid treatments, such as that used in this work to purify the arc-grown SWCNTs, are known to shorten the CNTs and induce defects on their side walls. Thus it is not striking that acid treated arc-grown based composites have lower E' than those including laser-grown SWCNTs. Further experiments would be required to determine the exact reason for the observed differences among the various samples. Our results do confirm the strong dependence of the mechanical properties of the composites on the CNTs synthesis method and post-treatments.

4. Conclusions

Different PEEK/SWCNT composites, at 0.1, 0.5 and 1 wt% SWCNT content, have been prepared by melt-blending. An efficient dispersion of the CNTs in the matrix was achieved by the combination of polymer ball milling and mechanical pre-treatments in ethanol, as revealed by SEM micrographs of fractured films. TGA thermograms show a substantial increase in the matrix degradation temperatures by the incorporation of SWCNTs. Higher thermal stability is found for samples with improved CNT dispersion. DSC experiments indicate a decrease in the crystallization temperature with

increasing SWCNT content, whereas the melting temperature remains almost constant. This behaviour can be explained by a confinement effect of the polymer chains within the CNT network, which delays the crystallization process and leads to lower values of T_c for the composites. No significant differences are found within the level of crystallinity of these composites calculated from DSC measurements. At room temperature, samples containing 0.1 wt% SWCNTs exhibit larger crystallite size than the raw matrix. At higher concentrations, the CNT network restricts the polymer chain diffusion and hinders the formation of large-size crystals. Furthermore, over the whole concentration range, composites including purified SWCNTs present bigger crystals. DMA studies reveal a non-linear growth in the storage modulus of the matrix by the addition of increasing SWCNT contents. This phenomenon can be attributed to weaker nanotube–matrix interfacial interactions taking place when a larger concentration regime is reached. SWCNTs restrict molecular mobility and consequently increase slightly the glass transition temperatures. The largest shift is found among composites with more homogeneous and fine distribution of the CNTs, that also exhibit enhanced rigidity, in particular those incorporating laser-grown SWCNTs, probably due to the improved quality and properties of this type of filler.

Acknowledgments

Financial support from a coordinated project between the National Research Council of Canada (NRC) and the Spanish National Research Council (CSIC) is gratefully acknowledged. Dr. A. Diez and Dr. M. Naffakh (I3PDR-6-02) would like to thank to Consejo Superior de Investigaciones Científicas (CSIC) for postdoctoral contracts. Partial support by the Spanish MICINN (national project MAT2006-13167-C01) is also acknowledged.

REFERENCES

- [1] Dai L, Mau AWH. Controlled synthesis and modification of carbon nanotubes and C_{60} carbon nanostructures for advanced polymeric composite materials. *Adv Mater* 2001;13(12–13):899–913.
- [2] Xie XL, Mai Y-W, Zhou X-P. Dispersion and alignment of carbon nanotubes in polymer matrix: a review. *Mater Sci Eng R* 2005;49(4):89–112.
- [3] Thostenson ET, Ren Z, Chou T-W. Advances in the science and technology of carbon nanotubes and their composites: a review. *Compos Sci Technol* 2001;61(13):1899–912.
- [4] Moniruzzaman M, Winey KI. Polymer nanocomposites containing carbon nanotubes. *Macromolecules* 2006;39(16):5194–205.
- [5] Enomoto K, Kitakata S, Yasuhara T, Ohtake N, Kuzumaki T, Mitsuda Y. Measurement of Young's modulus of carbon nanotubes by nanoprobe manipulation in a transmission electron microscope. *Appl Phys Lett* 2006;88(15):15315–7.
- [6] Yu M-F, Lourie O, Dyer MJ, Moloni K, Kelly TF, Ruoff RS. Strength and breaking mechanism of multiwalled carbon nanotubes under tensile load. *Science* 2000;287(5453):637–40.
- [7] Pop M, Mann D, Wang Q, Goodson K, Dai H. Thermal conductance of an individual single-wall carbon nanotube above room temperature. *Nano Lett* 2006;6(1):96–100.
- [8] Valter B, Ram MK, Nicolini C. Synthesis of multiwalled carbon nanotubes and poly(o-anisidine) nanocomposite material: fabrication and characterization of its Langmuir–Schaefer films. *Langmuir* 2002;18(5):1535–41.
- [9] Cadek M, Coleman JN, Barron V, Hedicke K. High-purity carbon nanotubes synthesis method by an arc discharging in magnetic field. *Appl Phys Lett* 2002;81(4):739–41.
- [10] Searle OB, Pfeiffer RH. Victrex[®] poly(ethersulfone) (PES) and Victrex[®] poly(ether ether ketone) (PEEK). *Polym Eng Sci* 1985;25(8):474–6.
- [11] Jones DP, Leach DC, Moore DR. Mechanical properties of poly(ether-ether-ketone) for engineering applications. *Polymer* 1985;26(9):1385–93.
- [12] Naffakh M, Gomez MA, Ellis G, Marco C. Thermal properties, structure and morphology of PEEK/thermotropic liquid crystalline polymer blends. *Polym Int* 2003;52(12):1876–86.
- [13] Cebe P, Chung SY, Hong SD. Effect of thermal history on mechanical properties of polyetheretherketone below the glass transition temperature. *J Appl Polym Sci* 1987;33(2):487–503.
- [14] Hsiung CM, Cakmak M, White JL. Crystallization phenomena in the injection molding of poly ether ether ketone and its influence on mechanical properties. *Polym Eng Sci* 1990;30(16):967–80.
- [15] Gojny FH, Wichmann MHG, Fieldler B, Bauhofer W, Schulte K. Influence of nano-modification on the mechanical and electrical properties of conventional fibre-reinforced composites. *Composites A* 2005;36(11):1525–35.
- [16] Thostenson ET, Chou TW. Carbon nanotube networks: sensing of distributed strain and damage for life prediction and self healing. *Adv Mater* 2006;18(21):2837–41.
- [17] Sandler J, Windle AH, Werner P, Altstadt V, Es MV, Shaffer MSP. Carbon-nanofibre-reinforced poly(ether ether ketone) fibres. *J Mater Sci* 2003;38:2135–41.
- [18] Sandler J, Werner P, Shaffer MSP, Demchuck V, Altstadt V, Windle AH. Carbon-nanofibre-reinforced poly(ether ether ketone) composites. *Composites A* 2002;33(8):1033–9.
- [19] Baaba M-R, Bantignies J-L, Alvarez L, Parent P, Le Normand F, Gulas M, et al. NEXAFS study of multi-walled carbon nanotubes functionalization with sulfonated poly(ether ether ketone) chains. *J Nanosci Nanotechnol* 2007;7(10):3463–7.
- [20] Journet C, Maser WK, Bernier P, Loiseau A, Lamy de la Chapelle M, Lefrant S, et al. Large-scale production of single-walled carbon nanotubes by the electric-arc technique. *Nature* 1997;388:756–8.
- [21] Blundell DJ, Osborn BN. The morphology of poly(aryl-ether-ether-ketone). *Polymer* 1983;24(8):953–8.
- [22] Dresselhaus MS, Dresselhaus G, Jorio A, Souza AG, Saito R. Raman spectroscopy on isolated single wall carbon nanotubes. *Carbon* 2002;40(12):2043–61.
- [23] Dresselhaus MS, Dresselhaus G, Saito R, Jorio A. Raman spectroscopy of carbon nanotubes. *Phys Rep* 2005;409(2):47–99.
- [24] Itkis ME, Perea D, Jung R, Niyogi S, Haddon RC. Comparison of analytical techniques for purity evaluation of single-walled carbon nanotubes. *J Am Chem Soc* 2005;127(10):3439–48.
- [25] Chen J, Hamon MA, Hu H, Chen Y, Rao AM, Eklund PC, et al. Solution properties of single-walled carbon nanotubes. *Science* 1998;282:95–8.
- [26] Pang LSK, Saxby JD, Chatfield SP. Thermogravimetric analysis of carbon nanotubes and nanoparticles. *J Phys Chem* 1993;97(27):6941–2.
- [27] Walker Jr PL. Carbon: an old but new material revisited. *Carbon* 1990;28(2–3):261–79.

- [28] Saxby JD, Chatfield SP, Palmisano AJ, Vassallo AM, Pang LSK. Thermogravimetric analysis of buckminsterfullerene and related materials in air. *J Phys Chem* 1992;96(1):17–8.
- [29] Ajayan PM, Schandler LS, Giannaris C, Rubio A. Single-walled carbon nanotube-polymer composites: strength and weakness. *Adv Mater* 2000;12(10):750–3.
- [30] Naffakh M, Ellis G, Gomez MA, Marco C. Thermal decomposition of technological polymer blends 1. Poly(aryl ether ether ketone) with a thermotropic liquid crystalline polymer. *Polym Degrad Stab* 1999;66(3):405–13.
- [31] Cao MY, Wunderlich B. A rheological study of long branching in polyethylene by blending. *J Polym Sci* 1985;23(2):521–7.
- [32] Chen G-X, Kim H-S, Park BH, Yoon J-S. Multi-walled carbon nanotubes reinforced nylon 6 composites. *Polymer* 2006;47(13):4760–7.
- [33] Xia H, Song M. Preparation and characterization of polyurethane-carbon nanotube composites. *Soft Matter* 2005;1(5):386–94.
- [34] Ge JJ, Hou H, Li Q, Graham MJ, Greiner A, Reneker DH, et al. Assembly of well-aligned multiwalled carbon nanotubes in confined polyacrylonitrile environments: electrospun composite nanofiber sheets. *J Am Chem Soc* 2004;126(48):15754–61.
- [35] Kim JY, Han SI, Kim DK, Kim SH. Mechanical reinforcement and crystallization behavior of poly(ethylene 2,6-naphthalate) nanocomposites induced by modified carbon nanotube. *Composites A* 2009;40(1):45–53.
- [36] Lee G, Jagannathan S, Choe HG, Minus ML, Kumar S. Carbon nanotube dispersion and exfoliation in polypropylene and structure and properties in the resulting composites. *Polymer* 2008;49(7):1831–40.
- [37] Bhattacharyya AR, Sreelumar TV, Liu T, Kumar S, Ericsson LM, Hauge RH. Crystallization and orientation studies in polypropylene/single wall carbon nanotube composite. *Polymer* 2003;44(8):2373–7.
- [38] Li L, Li CY, Ni C, Rong L, Hsiao B. Structure and crystallization behaviour of nylon 66/multi-walled carbon nanotube composites at low carbon nanotube contents. *Polymer* 2007;48(12):3452–60.
- [39] Naffakh M, Marco C, Gomez MA, Jiménez I. Unique isothermal crystallization behaviour of novel polyphenylene sulfide/inorganic fullerene-like WS₂ composites. *J Phys Chem B* 2008;112(47):14819–28.
- [40] Hay JN, Kemmish DJ, Langford JI, Rae AIM. The structure of crystalline PEEK. *Polym Commun* 1984;25:175–8.
- [41] Alexander LE, Krieger RE. X-ray diffraction methods in polymer science. New York: Wiley; 1969.
- [42] Mehta A, Isayev AI. The dynamic properties, temperature transitions, and thermal stability of poly(ether ether ketone)-thermotropic liquid crystalline polymer blends. *Polym Eng Sci* 1991;31(13):963–70.
- [43] Chae HG, Minus ML, Kumar S. Oriented and exfoliated single wall carbon nanotubes in polyacrylonitrile. *Polymer* 2006;47(10):3494–504.
- [44] Halpin JC, Kardos JL. The Halpin-Tsai equations: a review. *Polym Eng Sci* 1976;16(5):344–52.
- [45] Lu JP. Elastic properties of carbon nanotubes and nanoropes. *Phys Rev Lett* 1997;79(7):1297–300.
- [46] Lee B-L, Nielsen LE. Temperature dependence of the dynamic mechanical properties of filled polymers. *J Polym Sci B: Polym Phys* 1977;15(4):683–92.
- [47] Nielsen LE. Mechanical properties of polymers and composites, vol. 2. New York: Marcel Dekker; 1974.
- [48] Tsagaropoulos G, Eisenberg A. Dynamic mechanical study of the factors affecting the two glass transition behavior of filled polymers. Similarities and differences with random ionomers. *Macromolecules* 1995;28(18):6067–77.
- [49] Haskins RW, Maier RS, Ebeling RM, Marsh CP, Majure DL, Bednar AJ, et al. Tight-binding molecular dynamics study of the role of defects on carbon nanotube moduli and failure. *J Chem Phys* 2007;127(7):74708–18.